International Journal of Coal Science & Technology (2024) 11:28
https://doi.org/10.1007/s40789-024-00674-0

RESEARCH

Theoretical analysis of hydrogen solubility in direct coal liquefaction solvents

Xiaobin Zhang[1,2] · **Aoqi Wang**[1,2] · **Xingbao Wang**[1,2] · **Wenying Li**[1,2]

Received: 22 June 2023 / Revised: 15 September 2023 / Accepted: 4 March 2024

Abstract

The cyclic hydrogenation technology in a direct coal liquefaction process relies on the dissolved hydrogen of the solvent or oil participating in the hydrogenation reaction. Thus, a theoretical basis for process optimization and reactor design can be established by analyzing the solubility of hydrogen in liquefaction solvents. Experimental studies of hydrogen solubility in liquefaction solvents are challenging due to harsh reaction conditions and complex solvent compositions. In this study, the composition and content of liquefied solvents were analyzed. As model compounds, hexadecane, toluene, naphthalene, tetrahydronaphthalene, and phenanthrene were chosen to represent the liquefied solvents in chain alkanes and monocyclic, bicyclic, and tricyclic aromatic hydrocarbons. The solubility of hydrogen X (mol/mol) in pure solvent components and mixed solvents (alkanes and aromatics mixed in proportion to the chain alkanes + bicyclic aromatic hydrocarbons, bicyclic saturated aromatic hydrocarbons + bicyclic aromatic hydrocarbons, and bicyclic aromatic hydrocarbons + compounds containing heteroatoms composed of mixed components) are determined using Aspen simulation at temperature and pressure conditions of 373–523 K and 2–10 MPa. The results demonstrated that at high temperatures and pressures, the solubility of hydrogen in the solvent increases with the increase in temperature and pressure, with the pressure having a greater impact. Furthermore, the results revealed that hydrogen is more soluble in straight-chain alkanes than in other solvents, and the solubility of eicosanoids reaches a maximum of 0.296. The hydrogen solubility in aromatic ring compounds decreased gradually with an increase in the aromatic ring number. The influence of chain alkanes on the solubility of hydrogen predominates in a mixture of solvents with different mixing ratios of chain alkanes and aromatic hydrocarbons. The solubility of hydrogen in mixed aromatic solvents is less than that in the corresponding single solvents. Hydrogen is less soluble in solvent compounds containing heteroatoms than in compounds without heteroatoms.

Keywords Direct coal liquefaction · Liquefaction solvents · Process simulation · Hydrogen solubility

Direct coal liquefaction is a process in which the small molecules in coal pyrolysis are subjected to hydrogenation reactions to prepare high-performance liquid fuels (Shu et al. 1997; Shi 2012.; Qian et al. 2023) Since the solvent is pre-hydrogenated before entering the reactor, the amount of hydrogen dissolved in the liquefaction oil or solvent is crucial to the direct coal liquefaction hydrogenation technology (Shu 2009; Zhang 2006). Additionally, the solvent during liquefaction not only produces active hydrogen (Niu 2017) but also acts as a carrier for hydrogen storage by transferring hydrogen from coal and hydrogen (Pan et al. 2018; Niu et al. 2016). Furthermore, it has the effect of dissolving and dispersing coal and dissolving hydrogen (Niu et al. 2017; Gąsior and Smoliński 2022; Yan et al. 2021). However, harsh reaction conditions and solvents have a wide range of components (Guin et al. 1976; Gao et al. 2020), and differences between complex solvent compositions can alter the characteristics of solvents (Li et al. 2019a, b; Li et al. 2019a, b). All these factors impact hydrogen solubility, and in practice, industrial liquefaction solvents are mixtures of hydrogenated and stabilized liquefied medium-temperature solvents and high-temperature solvents in certain proportions (Li et al. 2022). At present, only a few studies have focused on how the differences in hydrogen solubility in

---

✉ Xingbao Wang
wangxingbao@tyut.edu.cn

[1] State Key Laboratory of Clean and Efficient Coal Utilization, Taiyuan University of Technology, Taiyuan 030024, Shanxi, China

[2] College of Chemical Engineering and Technology, Taiyuan University of Technology, Taiyuan 030024, China

solvents impact the performance of hydrogenation reactions (Bai et al. 2022; Wang et al. 2022). It is difficult to measure experimentally the solubility of hydrogen under high temperature and pressure conditions. It is challenging to experimentally analyze the effects of temperature, pressure, and solvent composition on the solubility of hydrogen due to the complex composition of liquefied solvents (Park et al. 1995, 1996; Brunner 1985).

The current research techniques on gas solubility mainly include experimental determination (Luo 2011; Yan 2020; Zhu et al. 2006) and modeling prediction (Humberto 2018; Saeid et al. 2016). The experimental determination methods include the equilibrium sampling method and the static analysis method, whereas the model-building prediction methods include the equation of state method and the activity coefficient method. To establish an optimization procedure for gas–liquid equilibrium data and subsequently to determine the parameters of the equation of state, Wiegand (1989) et al. used a modified cubic equation of state and binary interaction parameter mixing rule. To accurately predict the gas–liquid equilibrium data between oil and gas, the hydrogen solubility equilibrium constant prediction method was established after analyzing the gas–liquid equilibrium data of hydrogen in the kerosene model compounds. Harrison et al. (1985) determined the solubility of hydrogen in coal-liquefied oil and a four-component mixture of solvents at temperatures in the range of 125–400 °C and pressures up to 25 MPa. According to the results, the solubility of hydrogen in coal liquefaction oil increased as the temperature and pressure increased, and the variations in solubility were strongly related to the composition of the liquid-phase hydrocarbons. Luo (2011) analyzed the solubility of hydrogen in model compounds of coal liquefaction oil using the equilibrium sampling method, the results of which revealed that the solubility of hydrogen in alkanes was greater than that in aromatic hydrocarbons. Yan (2020) evaluated the solubility of hydrogen in tetrahydronaphthalene by the equilibrium sampling method. The findings revealed that the solubility of hydrogen in tetrahydronaphthalene increased with increasing temperature and hydrogen pressure. The relationship between hydrogen solubility and hydrogen partial pressure was almost linear.

In this study, the major focus was on the solubility of hydrogen in a few aromatic hydrocarbon compounds at relatively low temperatures and pressures. By analyzing the solvent, the results show that the solvent contains a large number of molecules with different properties. The structure and content of the molecules in different solvents vary, which can have an effect on hydrogen solubility. Since it is difficult to obtain these solvent compounds commercially, there is a lack of hydrogen solubility data for most solvents at high temperature and pressure conditions. The solubility of hydrogen is analyzed under high-temperature and high-pressure conditions in single-component and multi-component mixed solvents. Furthermore, the solubility of hydrogen in solvents under liquefaction process conditions was analyzed using Aspen Plus software calculations. The impact of temperature, pressure, and solvent composition on the solubility of hydrogen during the dissolution process was investigated. The work is instructive for the screening of solvents and selection of ratios for the process.

1 Experimental analysis

1.1 Materials

(1) Raw materials: the medium-temperature solvent fractions (220–350 °C) and the high-temperature solvent fractions (> 350 °C) obtained from Shenhua Coal to Oil Chemical Co. were separated by hydrogenation and stabilization. The elemental analyses are shown in Table 1. This table shows that the H/C of the two solvents are similar, the O and S contents of the medium temperature solvent are higher than that of the high temperature solvent, the N content of the medium-temperature solvent is higher than that of the high-temperature solvent, the H content of the high-temperature solvent is higher than that of the medium-temperature solvent, and the C contents of the two solvents are similar.

(2) Reagents: The reagents used in the analytical experiments are n-hexane, dichloromethane, and anhydrous ethanol.

(3) Instruments: The solvents were analyzed using a Fourier transform infrared spectrometer (Bruker), a synchronous fluorescence spectrophotometer (Varian), and comprehensive two-dimensional gas chromatography (Shimadzu).

Table 1 Elemental analysis of medium and high temperature solvents

Solvents type	Elemental Analysis (wt%)					H/C
	N	C	H	S	O	
Medium temperature solvent	0.58	85.73	8.98	0.12	1.91	0.10
High temperature solvent	0.52	85.76	9.09	0.07	1.43	0.11

1.2 Solvent analysis

In this paper, the types and contents of the elements contained in the solvent were first analyzed. The CHNS mode and O mode of the elemental analyzer were applied for the determination, respectively. The functional group information of the molecular structure of the solvent (Mu 2018) and the type of functional groups contained in the solvent are determined using Fourier transform infrared spectroscopy. The aromaticity of the solvent, the number of aromatic rings in the solvent, and their classification are determined using simultaneous fluorescence spectroscopy. As a consequence of the limitation presented by the inlet gasification temperature of GC × GC–MS/FID and the column-withstanding temperature, it is difficult to volatilize the high boiling point component and is likely to block the column. Hence, the solvent below the boiling point of 350 °C is detected, and a relatively accurate quantitative analysis is performed. The results are relatively accurate and quantitative. The results of the analysis of the compound composition, molecular structure, and content in solvents are crucial in the detailed study of the factors influencing the solubility of hydrogen.

1.3 Results of solvent analysis

1.3.1 Infrared spectroscopy of solvents

Figure 1 illustrates the IR absorption spectra of the medium- and high-temperature solvents. Both solvents exhibit a strong absorption peak at 2933 cm^{-1}, which is the stretching vibration absorption peak of CH_3, indicating that both solvents contain the CH_3 functional group. A sharp and strong absorption peak is observed at 2853 cm^{-1}, which is the symmetric stretching vibration of CH_2, suggesting the presence of carbon chains in both solvents. Both solvents contain alkanes with various carbon chain lengths, as depicted by the peak at 2853 cm^{-1}, which is a symmetric stretching vibration of CH_2. A broad absorption band near 3126 cm^{-1} indicates that the molecular structure undergoes O–H stretching vibration and N–H stretching vibration and that both solvents may contain compounds that contain heteroatoms. A strong absorption peak is observed near 1400 cm^{-1} with the C-H bending vibration of alkanes. The presence of aromatic hydrocarbon structures in both solvents is indicated by a small and sharp peak with a benzene ring skeleton vibration absorption peak at 1604 cm^{-1} for both solvents. A certain amount of aromatic compounds containing substituents, mainly short-side chain substituents, are present in both solvents, as demonstrated by the stretching vibration absorption peak of aromatic substituents in the range of 650–910 cm^{-1}.

1.3.2 Simultaneous fluorescence spectroscopy of solvents

Figure 2 displays the simultaneous fluorescence spectra of the two solvents, and characteristic peaks are observed at the peak positions of the spectra (Mu 2018). Monocyclic and bicyclic aromatic hydrocarbons with high content predominate in the range of 270–340 nm in the medium-temperature solvent. Moreover, there are certain small peaks after 340 nm, indicating that there are small amounts of tricyclic and more than tricyclic aromatic hydrocarbons in the solvent. When compared to the medium-temperature solvent, the high-temperature solvent has distinct characteristic peaks in the ranges of 270–340 nm, 340–370 nm, and 370–400 nm, which indicates the presence of tricyclic, tetracyclic and tetracyclic aromatic compounds in addition to monocyclic and bicyclic aromatic compounds.

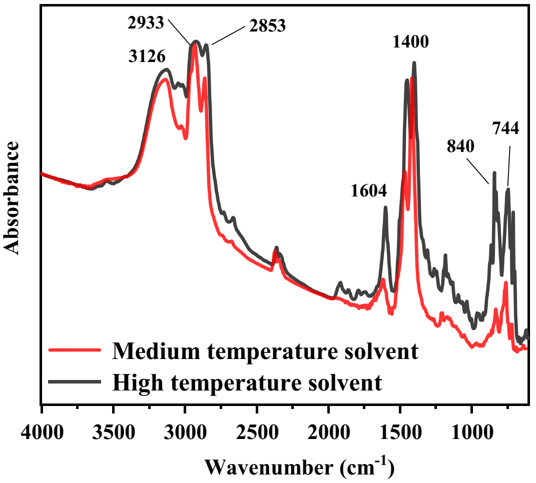

Fig. 1 Infrared absorption spectra of medium- and high-temperature solvents

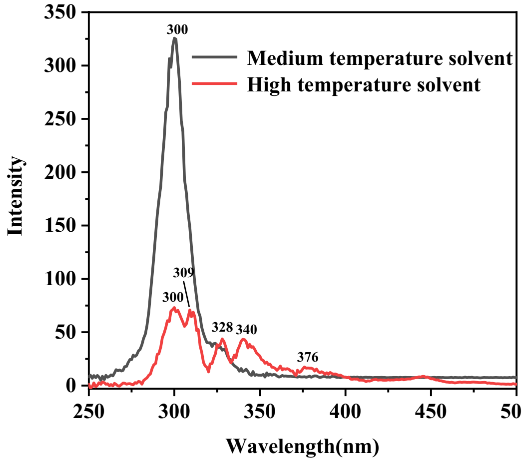

Fig. 2 Synchrotron fluorescence spectra of medium and high temperature solvents ($\Delta\lambda = 14$ nm)

1.3.3 Solvent composition and structural analysis

Figure 3 illustrates the full two-dimensional chromatogram of the medium-temperature solvent. According to the qualitative analysis of the solvent, it is primarily composed of chain alkanes, cycloalkanes, and aromatics. It is observed from the figure that the solvent is arranged from left to right in order of its lowest to highest carbon number, with the distribution of chain alkanes at the bottom and the carbon number increasing from left to right. They are arranged as chain alkanes, cycloalkanes, and aromatics from bottom to top. From left to right, they are divided into monocyclic, bicyclic, tricyclic, and tetracyclic aromatic compounds.

According to the analysis of the components in the solvents, medium-temperature solvents contained mostly bicyclic hydrocarbons, accounting for 35.42% of the total compounds in the solvents. This was followed by tricyclic hydrocarbons, which account for 23.75% of the total compounds in the solvents, and the least amount of the compounds were monocyclic hydrocarbons, which account for 3.35% of the total compounds.

2 Process simulation

2.1 Establishment of simulation process

The simulation process of hydrogen solubility must be established for Aspen Plus simulation calculations. When the pressure of the gas–liquid mixture system is reduced in the flash separation module, the gas dissolved in the solvent undergoes rapid desorption to release it, forming a flash separation process. During the simulation, any two of the following four parameters must be specified: temperature, heat load, pressure, and gas phase fraction. In this study, the flash operation was an adiabatic flash with a heat load of 0.

2.2 Selection of equation of state

The selection of different equations of state considerably impacts the calculation results in Aspen Plus simulations. The property methods recommended for calculations in petrochemical systems include PR (Peng-Robinson), RK-SOAVE (Redlich Kwong SOAVE), and GRAYSON. In gas–liquid equilibrium system calculations, the PR, SRK (Soave Redlich Kwong), and PSRK (Peng Soave Redlich Kwong) methods are recommended (Sun et al. 2012). However, there is no set recommended method for the analysis of hydrogen solubility in the direct coal liquefaction process.

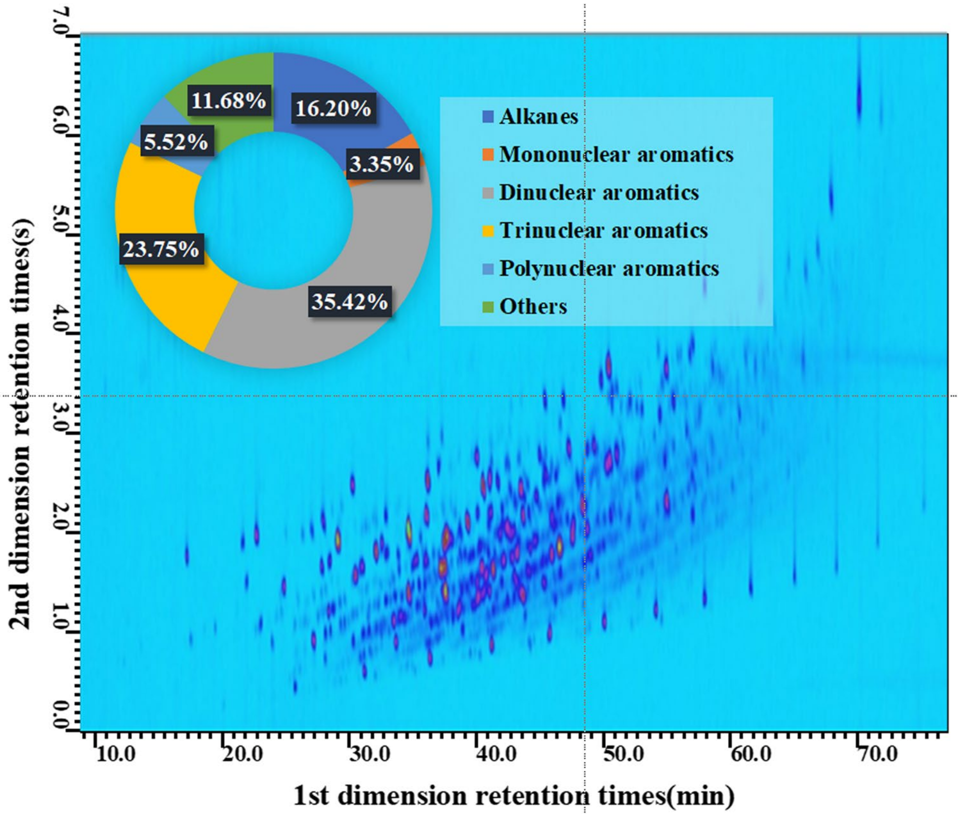

Fig. 3 Two-dimensional contour plot of medium-temperature solvents

Therefore, in this study, the solubility of hydrogen in hexadecane, toluene, naphthalene, and phenanthrene was calculated using the aforementioned physical property methods.

The specific operating conditions set in Aspen Plus are as follows: Hydrogen and solvent are set as feed components; feed temperature is selected from the range of 373–453 K; pressure is chosen from the range of 2–20 MPa; the hydrogen feed rate is 1 kmol/h; and the solvent feed rate is 1 kmol/h. The operating conditions of the flash separation module are set at the same temperature as the material conditions, and the pressure is lower than the material feed conditions for the calculation of flash separation. Due to the moderate conditions of the current experiment. Therefore, in this paper, a range of temperatures and pressures were chosen to ensure the reliability of the simulation method developed. In the subsequent study, the temperature and pressure closer to the actual industry will be used for simulation to provide some guidance for the actual process.

Figure 4 displays the hydrogen solubility calculated using different equations of state and the experimentally measured values of hydrogen solubility (Park et al. 1995; Luo 2011). The results reveal that the values of hydrogen solubility obtained from simulations using the SRK equation of state are close to the experimental values, with an average deviation of less than 5%. Furthermore, it demonstrates that the SRK equation of state is suitable for the simulation of hydrogen solubility in liquefied solvents.

2.3 State equation model parameters in aspen plus

The solubility of the gas in the liquid phase is often determined by using activity coefficients in the equation of state

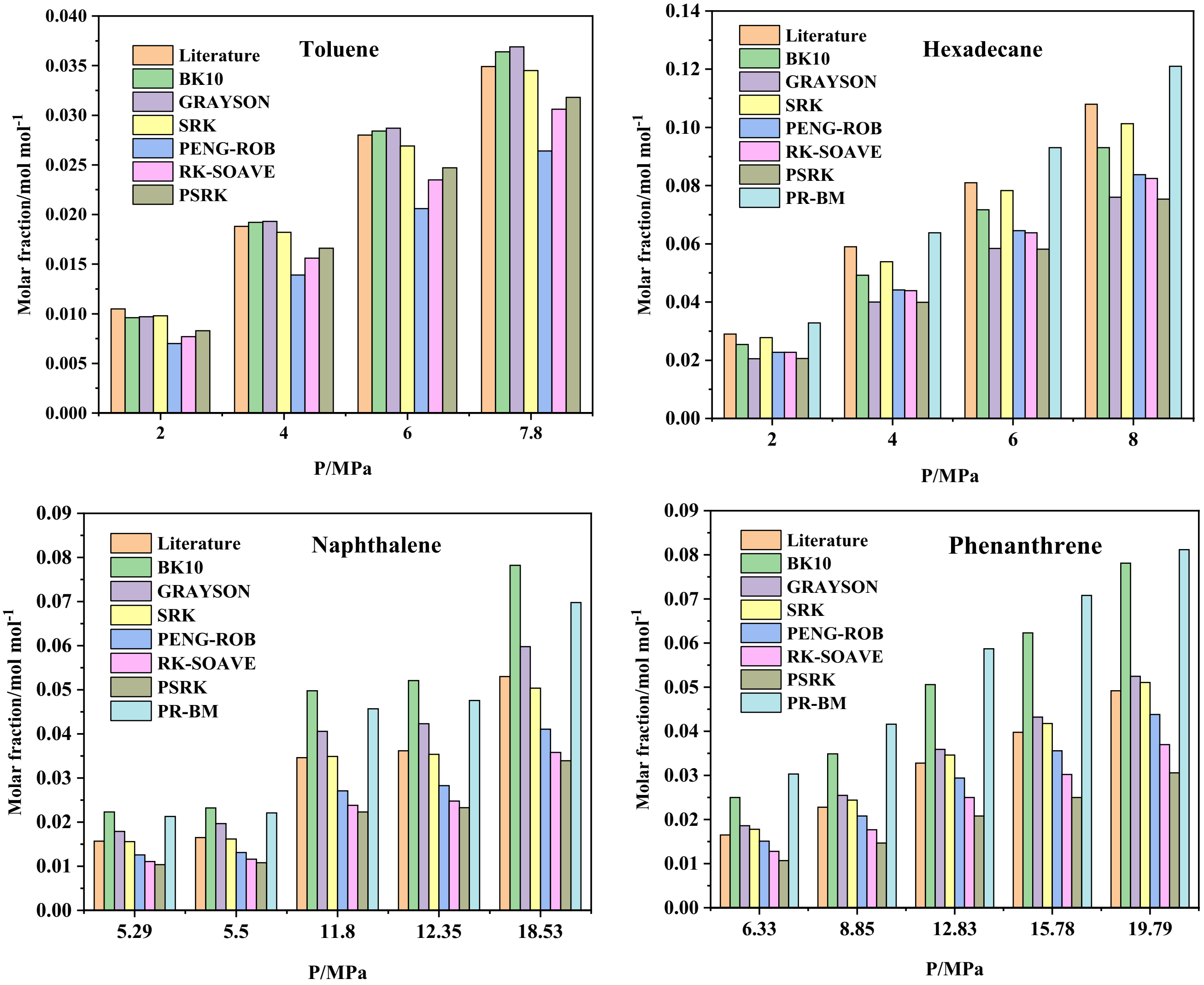

Fig. 4 Comparison of hydrogen solubility in toluene, n-hexadecane, naphthalene and phenanthrene at different pressures between calculation and experimental data

method (Mao 2012; Wang et al. 2015). Besides, the criterion for gas–liquid phase equilibrium is that the gas-phase escape of the solvent must be equal to the liquid-phase escape. Equation (1) represents the SRK equation of state, where *P* and *T* denote the state pressure and temperature, respectively, and Vm denotes the molar volume of the gas.

$$P_2 = \frac{RT_2}{V_\mathrm{m} - b} - \frac{a(T_2)}{V_\mathrm{m}(V_\mathrm{m} + b)} \tag{1}$$

The term $\frac{RT_2}{V_\mathrm{m}-b}$ represents the repulsive term and $\frac{a(T_2)}{V_\mathrm{m}(V_\mathrm{m}+b)}$ represents the gravitational term.

The equation of state method can be used with the aid of the built-in physical property database in Aspen Plus, which includes the physical property methods for most chemical reactions and the physical parameters of numerous components, such as critical temperature and critical pressure. For the study of gas–liquid equilibrium and gas–liquid equilibrium constants, system state parameters and parameters of phase property changes are crucial in addition to temperature-related thermodynamic parameters (Yang and Feng 2009).

2.4 Model validation

Given that the composition of liquefied solvents contains a significant amount of compounds with aromatic structures and also some chain hydrocarbon compounds, it is necessary to verify the reliability of the hydrogen solubility calculation model at different temperatures and pressures. Therefore, in this study, the solubility of hydrogen in n-decane and toluene at different temperatures and pressures was calculated. The relative errors of the solubility calculation values were found to be less than 10%, indicating the reliability of the established calculation models. Table 2 displays the results. For temperatures of 298 K (293 K in n-decane), 323 K, and 373 K, and pressures of 2–8 MPa, the calculated values of hydrogen solubility in toluene were close to the experimental values (Brunner 1985), with an average deviation of 4%. Moreover, the calculated values of hydrogen solubility in n-decane were close to the literature values (Brunner 1985), with an average deviation of 5%. Therefore, Aspen Plus software and the SRK equation of state were utilized to accurately study the solubility of hydrogen in solvents across a wide range of temperatures and pressures.

Table 2 Comparison of hydrogen solubility in toluene and decane at different temperatures between calculation and experimental data (Brunner 1985)

Item	Sim (mol%)	Exp (mol%)	Relative error (%)	Item	Sim (mol%)	Exp (mol%)	Relative error (%)	Item	Sim (mol%)	Exp (mol%)	Relative error (%)
P (MPa)	298 K			*P* (MPa)	323 K			*P* (MPa)	373 K		
Toluene											
2	0.59	0.68	−13.1	2	0.7	0.78	−10.6	2	0.92	1.05	−12.4
4	1.17	1.22	−4.4	4	1.38	1.32	4.2	4	1.82	1.88	−3.4
6	1.73	1.65	4.6	6	2.03	1.82	11.8	6	2.69	2.80	−4.0
8	2.27	2.21	2.7	8	2.68	2.45	9.2	8	3.45	3.49	−1.1
Decane											
P (MPa)	293 K			*P* (MPa)	323 K			*P* (MPa)	373 K		
2.37	1.56	1.58	−1.0	2.82	2.08	2.22	−6.3	2.04	1.88	2.04	−8.0
2.38	1.57	1.58	−0.6	5.64	4.04	4.36	−7.3	4.69	4.18	4.62	−9.4
10.35	6.33	6.66	−4.9	9.42	6.51	7.04	−7.6	9.4	7.96	8.85	−10.1

3 Analysis of influencing factors

3.1 Effect of temperature and pressure on the solubility of hydrogen

Based on the results of solvent analysis, tetrahydronaphthalene was screened as a pure component solvent model compound to study the effect of temperature and pressure on hydrogen solubility in the pure component solvent. The solubility of hydrogen increases with pressure mainly because as pressure increases, the concentration of the gas phase increases. This breaks the original gas–liquid equilibrium and shifts it to the right, and hydrogen dissolves more readily in the solvent. As the pressure rises, the surface tension of the liquid decreases, which enables the gas molecules to enter the liquid phase through the gas–liquid interface. The hydrogen solubility increases with temperature, the gravitational interaction between the molecules becomes weaker, and the surface tension of the liquid decreases (Luo 2011). Meanwhile, the vapor partial pressure of the solvent in the high-temperature phase increases with the increase in temperature. As a result of the increased gas pressure in the gas phase, the solubility of hydrogen in the solvent increases.

A two-component mixed solvent model compound of tetrahydronaphthalene + hexadecane (1:1 molar ratio) was chosen to investigate the effect of temperature and pressure on the solubility of hydrogen. Additionally, the relationship between the composition of liquefied solvents and the solubility of hydrogen is analyzed. As per the findings, the solubility of hydrogen in the mixed solvent gradually increased with the increase in temperature and pressure. As observed in Fig. 5b, hydrogen is more soluble in the mixed solvent of tetralin + hexadecane at the same temperature and pressure than it was in the pure component tetralin, indicating that

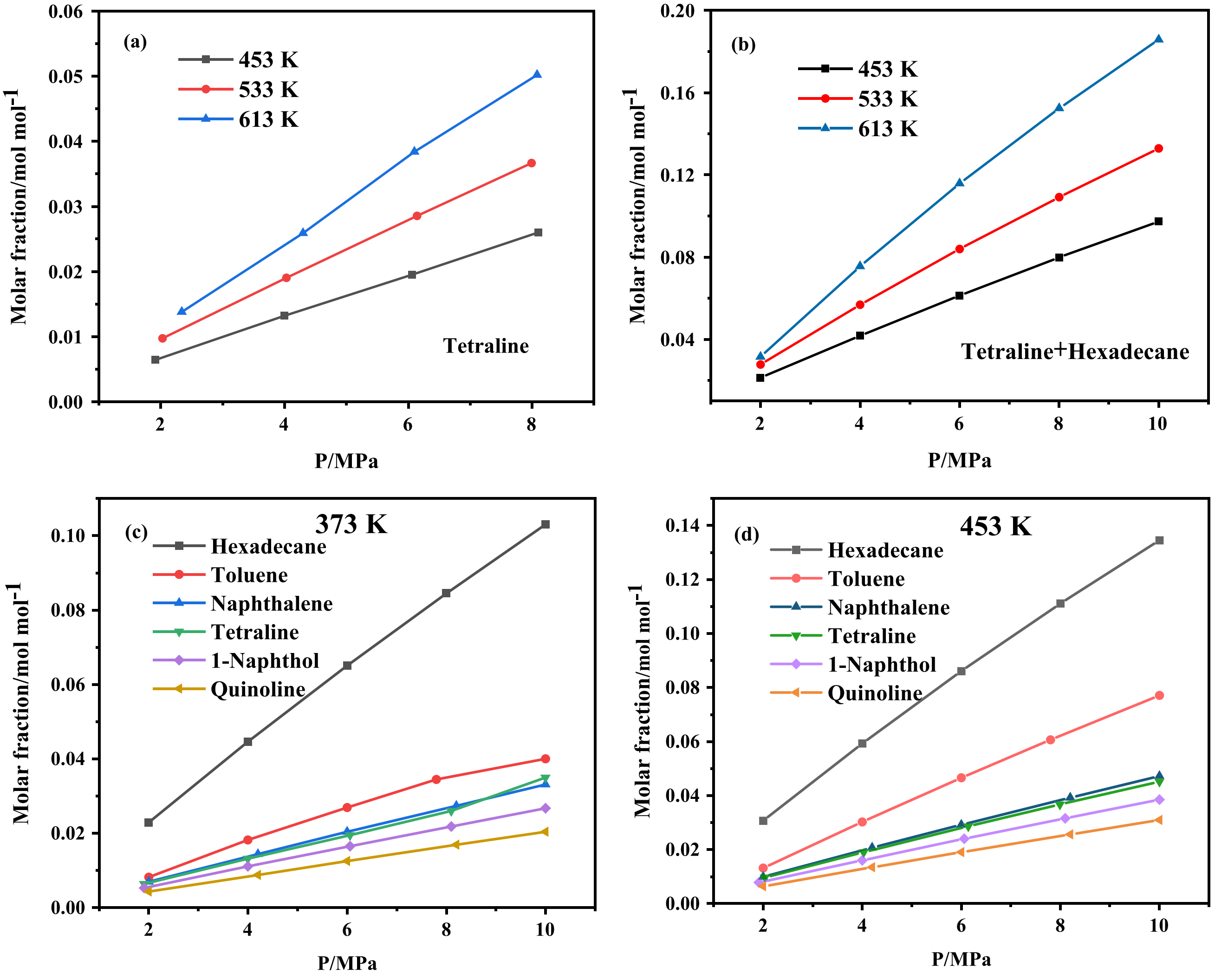

Fig. 5 Comparison of hydrogen solubility in single solvent (**a**, **c**, **d**) and **b** mixed solvents at different temperatures and pressures

the content of chain alkanes in the mixed solvent played an important role in the amount of hydrogen dissolved.

On further analyzing Fig. 5, it is observed that at higher temperatures, the increase in the slope of the straight line is less evident, and the solubility increase presents a gradually decreasing trend. Furthermore, the increase in hydrogen solubility becomes less obvious as the temperature rises. The increase in hydrogen solubility slows down since, at high temperatures, the motion of gas molecules intensifies, the collision frequency between hydrogen bubbles increases, and the small bubbles merge into large bubbles, which is non-conducive to the mass transfer of hydrogen in the liquid phase.

3.2 Dissolution pattern of hydrogen in pure component solvents

It is observed from Fig. 5c and d that the solubility of hydrogen varies at the same temperature and pressure in different solvents. This presents a solubility pattern in which the solubility of hydrogen is significantly greater in chain alkanes than in other solvents and greater in monocyclic aromatic hydrocarbons than in polycyclic aromatic hydrocarbons. Besides, there is a slight difference in solubility between fully unsaturated aromatic hydrocarbons and partially hydrogenated aromatic hydrocarbons and significantly lower solubility in nitrogen- or oxygen-containing heteroatom compounds than in other heteroatom-free hydrocarbons.

3.3 The dissolution law of hydrogen in mixed solvents

This study presents the solubilities of hydrogen in hexadecane + tetralin, quinoline + tetralin, and hexadecane + 1-naphthol (different mass fractions) at 453 K under different pressures to study the impact of the composition of different solvent mixtures on the solubility of hydrogen. Figure 6 displays the results.

As depicted in Fig. 6a, the solubility of hydrogen in the mixture of hexadecane + tetralin decreases gradually as the tetralin content increases at the same temperature and pressure. This indicates that when chain alkanes and aromatics are used as the mixture solvent, the size of hydrogen solubility depends on the chain alkanes. The lower the content of tetralin and the higher the content of hexadecane in the mixture solvent, the greater the solubility of hydrogen. It is evident from Fig. 6b that at the same temperature and pressure, the increase in the solubility of hydrogen in the mixture is more pronounced with the increase in the tetralin content in the mixture of quinoline and tetralin. The size of the hydrogen solubility in this mixture depends on the tetralin content. In the mixture of hexadecane and 1-naphthol, the solubility of hydrogen in the mixture of solvents decreased (see Fig. 6c) with the increase in the 1-naphthol content at the same temperature and pressure. According to the aforementioned findings, the difference in hydrocarbon content, of which the chain alkanes have a greater influence, is the decisive factor that causes the variations in hydrogen solubility in the mixed solvents at the same temperature and pressure.

The solubility of hydrogen in a mixture of two components was investigated by studying the impacts of naphthalene and quinoline on hydrogen solubility in these mixtures. Furthermore, the effect of the content of other components on the solubility of hydrogen in the mixture when the mass fraction of one of the components is the same was explored.

Figure 7 shows that the solubility of hydrogen in hexadecane + naphthalene and that in hexadecane + quinoline are close to each other when the mass fraction of hexadecane in the solvent mixture is the same at a temperature of 453 K and pressure in the range of 2–4 MPa. The solubility of hydrogen in hexadecane + naphthalene and that in

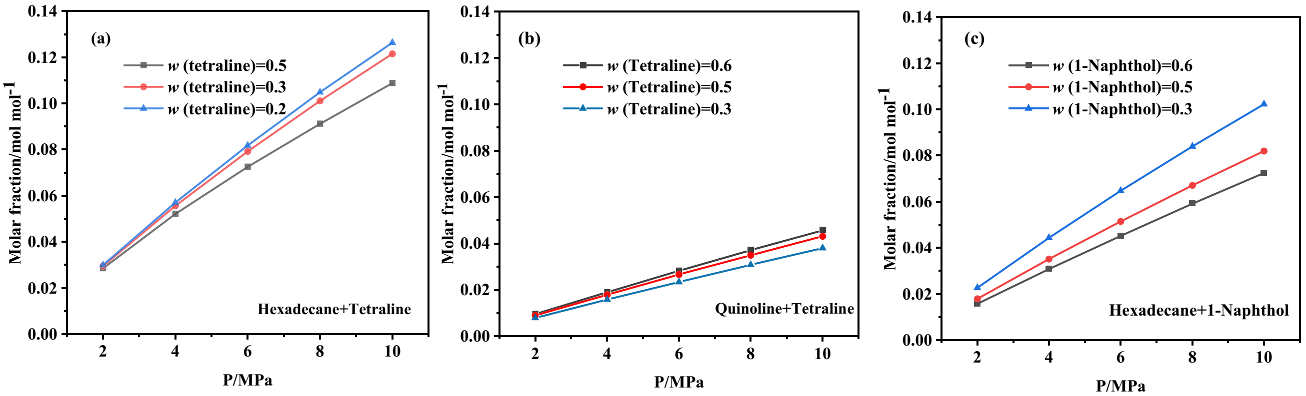

Fig. 6 Hydrogen solubility in the mixture of different concentrations of **a** hexadecane + tetralin, **b** quinoline + tetralin and **c** hexadecane + 1–naphthol at 453 K

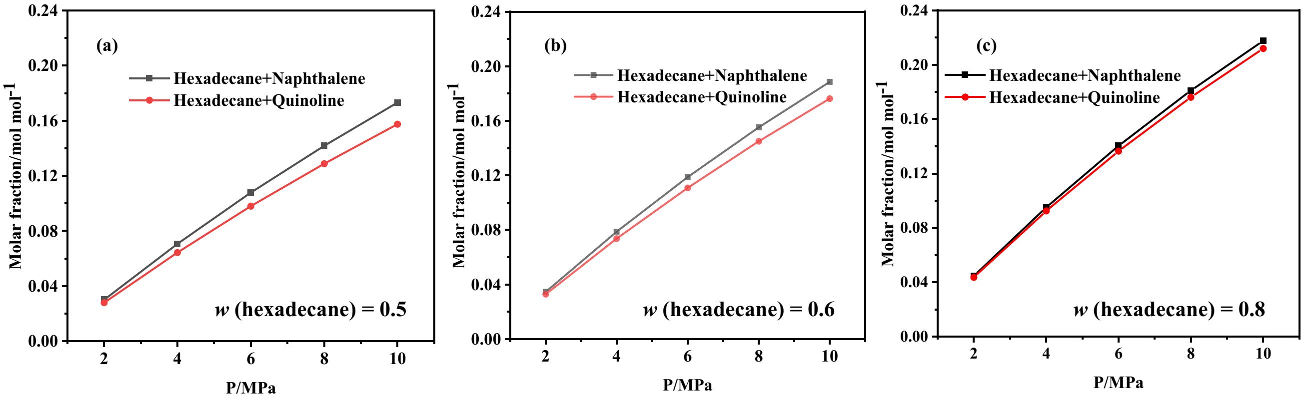

Fig. 7 Hydrogen solubility in the mixture of different concentrations of hexadecane + naphthalene and quinoline at 453 K; ω (hexadecane) = **a** 0.5, **b** 0.6, **c** 0.8

hexadecane + quinoline is almost the same under this condition when the mass fraction of hexadecane is higher in the solvent mixture. However, the solubility of hydrogen in hexadecane + naphthalene is greater than that in hexadecane + quinoline when the temperature is kept constant, and the pressure is in the range of 4–10 MPa.

Dissolution consists of three main processes related to free energy: first, a cavity will be formed in the solvent molecule that can hold the solute molecule (absorbing heat); second, the solute molecules will separate from each other and enter the cavity (releasing heat); and third, the solute molecule and solvent molecule will interact with each other. For the dissolution process of hydrogen in the solvent, it is mainly reflected in the solvent molecules first form a space that can accommodate the solute molecules, and then the solute molecules enter into the space formed by the solvent molecules, and at the same time, there is a certain interaction between the solute molecules and the solvent molecules in this process(Chen et al. 1996).

4 Conclusions

Based on the results of solvent analysis, the hydrogen dissolution law and the amount of dissolution in various components of coal direct liquefaction solvents were analyzed, and the following conclusions were obtained:

(1) The liquefied medium-temperature solvent contains mostly bicyclic compounds, whereas the high-temperature solvent contains more tricyclic and tetracyclic compounds than the medium-temperature solvent. All the solvents contain some amount of straight-chain alkanes, and the cyclic compounds in the solvent are primarily concentrated in 2–4 rings.

(2) The effects of temperature and pressure, as well as solvent composition, on the solubility of hydrogen in solvents were examined through a research method. The solubility of hydrogen in the solvent was found to increase with increasing temperature and pressure, and this relationship is linear. Moreover, the solubility of hydrogen tended to decrease gradually at higher temperatures with increasing pressure, and the effect of temperature on the increase in hydrogen solubility was weaker than that of hydrogen pressure.

(3) The solubility of hydrogen in chain alkanes is higher than that in other solvents, and the solubility of hydrogen in the mixed solvent of chain alkanes and aromatics is stronger than that in the single-component aromatic solvent. Besides, the solvent molecules containing heteroatoms are non-conducive to the increase in hydrogen solubility, and the increase in the chain alkane content in the mixed solvent will promote the solubility of hydrogen.

Author contributions XZ and XW, Conceptualization, Methodology and Writing – original draft. XZ, AW, and XW, Writing – original draft. XW and WL, Review and editing.

Funding The authors are very grateful for the financial support from the National Key Research and Development Program of China (2022YFB4101302-01), the National Natural Science Foundation of China (22178243) and the science and technology innovation project of China Shenhua Coal to Liquid and Chemical Company Limited (MZYHG-22–02).

Declarations

Conflict of interest The authors declare that they have no conficts of interest.

References

Bai JK, Zhang XB, Li W, Wang XB, Du ZY, Li WY (2022) Rate constant of hydrogen transfer from H–donor solvents to coal radicals. Fuel 318:123621. https://doi.org/10.1016/j.fuel.2022.123621

Brunner E (1985) Solubility of hydrogen in 10 organic solvents at 298.15, 323.15, and 373.15 K. J Chem Eng Data 30:269–273. https://doi.org/10.1021/je00041a010

Chen JW, Liu F, Liao YY et al (1996) Using AMI hamiltonian in quantitative structure-properties relationship studies of Alkyl(1-Phenylsulfonyl)cycloalkane-carboxylates. Chemosphere 33(3):537–546. https://doi.org/10.1016/0045-6535(96)00197-X

Gao SS, Li QH, Shu GP, Wu JP (2020) Molecular composition and distribution characteristics of saturated hydrocarbons in direct coal liquefaction circulating solvent. Coal Convers 43(2):17–25. https://doi.org/10.19726/j.cnki.ebcc.202002003

Gąsior R, Smoliński A (2022) Use of coals and wastes in a co-gasification process aimed at producing hydrogen rich gas. Int J Coal Sci Technol 9(1): 82. https://doi.org/10.1007/s40789-022-00548-3

Guin J, Tarrer A, Taylor L, Prather J, Green S (1976) Mechanisms of coal particle dissolution. Ind Eng Chem Process Des Dev 15(4):490–494. https://doi.org/10.1021/i260060a003

Harrison RH, Scheppele SE, Sturm GP et al (1985) Solubility of hydrogen in well–defined coal liquids. J Chem Eng Data 30(2):183–189. https://doi.org/10.1021/je00040a016

Humberto A-C (2018) Predictive method of hydrogen solubility in heavy petroleum fractions using EOS/GE and group contributions methods. Fuel 224:619–627. https://doi.org/10.1016/j.fuel.2018.03.116

Li WY, Mu H, Wang W, YE CP, Feng J (2019a) Status quo and out–look of qualitative and quantitative analysis of light weight fractions of coal–based crude oil. Chem Ind Eng Progress 38(1):217–228. https://doi.org/10.16085/j.issn.1000-6613.2018-0887

Li WY, Wang W, Mu H, Li W, Ye CP, Feng J (2019b) Analysis of light weight fractions of coal–based crude oil by gas chromatography combined with mass spectroscopy and flame ionization detection. Fuel 241:392–401. https://doi.org/10.1016/j.fuel.2018.12.045

Li HJ, Zhang XB, Wang XB, Li WY (2022) Research progress and prospects of coal direct liquefaction solvents. J China Coal Soc 47(10):3791–3804. https://doi.org/10.13225/j.cnki.jccs.2021.1404

Lin Q, Jinkai X, Chao T, Chao M, Xiaopeng J, Feiqiang G (2019) Effect of demineralization on pyrolysis characteristics of LPS coal based on its chemical structure. Int J Coal Sci Technol 10(1): 21. https://doi.org/10.1007/s40789-023-00576-7

Luo HF (2011) The regular pattern of hydrogen dissolved in coal liquid and role of hydrogen for quick coal liquefaction at high temperature. Taiyuan University of Technology, Taiyuan. https://doi.org/10.7666/d.d196787

Mao XF (2012) Application of PSRK-UNIFAC model in vapor-liquid equilibria prediction under high temperatures and pressures during coal direct liquefaction. Clean Coal Technol 18(3):53–58. https://doi.org/10.13226/j.issn.1006-6772.2012.03.017

Mu H (2018) Qualitative and quantitative study on coal-based crude oil constrained by material balance. Taiyuan University of Technology, Taiyuan

Niu B (2017) Role of solvents and hydrogen transfer mechanism in direct coal liquefaction. Dalian University of Technology, Dalian

Niu B, Jin LJ, Li Y, Shi ZW, Yan HX, Hu HQ (2016) Interaction between hydrogen–donor and nondonor solvents in direct liquefaction of bulianta coal. Energy Fuels 30(12):10260–10267. https://doi.org/10.1021/acs.energyfuels.6b02223

Niu B, Jin LJ, Li Y, Shi ZW, Li YT, Hu HQ (2017) Mechanism of hydrogen transfer and role of solvent during heating–up stage of direct coal liquefaction. Fuel Process Technol 160:130–135. https://doi.org/10.1016/j.fuproc.2017.02.026

Pan H, Bai ZQ, Zhao ZT, Hao P, Ge ZF, Hou RR, Bai J, Guo ZX, Kong LX, Li W (2018) Role of hydrogen donor and non–donor binary solvents in product distribution and hydrogen consumption during direct coal liquefaction. Fuel Process Technol 173:75–80. https://doi.org/10.1016/j.fuproc.2018.01.012

Park J, Robinson RL, Gasem K (1995) Solubilities of hydrogen in heavy normal paraffins at temperatures from 3232 to 4232 K and pressures to 174 MPa. J Chem Eng Data 40(1):241–244. https://doi.org/10.1021/je00017a051

Park J, Robinson RL, Gasem K (1996) Hydrogen solubility in aromatic hydrocarbon from 323 to 433 K and pressures to 21.7 MPa. J Chem Eng Data 41:70–73. https://doi.org/10.1021/je950152n

Saeid N, Ali B-H, Afshin T et al (2016) Accurate prediction of solubility of hydrogen in heavy oil fractions. J Mol Liq 222:933–943. https://doi.org/10.1016/j.molliq.2016.07.083

Shi SD (2012) Engineering fundamental of direct coal liquefaction. Chemical Industry Press, Beijing, pp 44–56

Shu GP (2009) Development history and its significance of shenhua coal direct liquefaction. Shen Hua Sci Technol 7(1):78–82. https://doi.org/10.3969/j.issn.1674-8492.2009.01.015

Shu GP, Xu ZG (1997) Direct coal liquefaction technology. China. Coal 23(10):21–23+59. https://doi.org/10.19880/j.cnki.ccm.1997.10.006

Sun LY (2012) Chemical engineering process simulation using Aspen Plus. Chemical Industry Press. ISBN: 9787122145536

Wang CJ, Ma ST, Cheng ZM (2015) Fitting binary interaction parameter of PR EOS and predicting hydrogen solubility in diesels. Comput Appl Chem 32(5):556–560. https://doi.org/10.11719/com.app.chem20150508

Wang XB, Bai JK, Zhang XB, Li W, Du ZY (2022) The mechanism and rate constant of hydrogen transfer from solvent radicals to coal–based model compounds in direct coal liquefaction. J Anal Appl Pyrol 167:105637. https://doi.org/10.1016/j.jaap.2022.105637

Wiegand KW, Strobel D, Hofmann H (1989) Vapour–liquid equilibria of hydrogen/coal liquid and methane/coal liquid systems at elevated temperatures and pressures. Chem Eng Technol 12(1):280–288. https://doi.org/10.1002/ceat.270120139

Yan B (2020) Dissolution behavior of hydrogen in the recycle solvent of mild coal direct liquefaction. Beijing University of Chemical Technology, Beijing. https://doi.org/10.26939/d.cnki.gbhgu.2020.001669

Yan B, Zhang G, Gao P, Li H, Ren SH, Wu WZ (2021) Dissolution behavior of hydrogen in the model recycle solvent of mild direct coal liquefaction. Fuel Process Technol 223:106982. https://doi.org/10.1016/j.fuproc.2021.106982

Yang CX, Feng J (2009) Vapor—liquid equilibrium of coal liquefied oil fractions under high temperature and high pressure. J Fuel Chem Technol 37(3):271–276. https://doi.org/10.7666/d.y1306585

Zhang YZ (2006) New progress of china shenhua coal direct liquefaction technology. China Energy Sci Technol 2:32–35

Zhu TX, Ling KC, Shen J, Wang YC, Zhang HJ (2006) Solubilities of hydrogen in coal liquefied oil. Coal Conversion 29(3):32–36. https://doi.org/10.3969/j.issn.1004-4248.2006.03.008